LETTER

Diffusion of a Brownian ellipsoid in a force field

A Letters Journal Exploring the Frontiers of Physics

May 2016

EPL, **114** (2016) 30005
doi: 10.1209/0295-5075/114/30005

www.epljournal.org

Diffusion of a Brownian ellipsoid in a force field

Erik Aurell[1,2], Stefano Bo[3], Marcelo Dias[3,4], Ralf Eichhorn[3(a)] and Raffaele Marino[3]

[1] *Department of Computational Biology and Center for Quantum Materials, KTH - Royal Institute of Technology, AlbaNova University Center - SE-106 91 Stockholm, Sweden*
[2] *Departments of Information and Computer Science and Applied Physics, Aalto University - Espoo, Finland*
[3] *Nordita, Royal Institute of Technology and Stockholm University - Roslagstullsbacken 23, SE-106 91 Stockholm, Sweden*
[4] *Aalto Science Institute, School of Science, Aalto University - FI-02150 Espoo, Finland*

received 12 February 2016; accepted in final form 14 May 2016
published online 1 June 2016

PACS 05.40.Jc – Brownian motion
PACS 05.70.Ln – Nonequilibrium and irreversible thermodynamics
PACS 05.40.-a – Fluctuation phenomena, random processes, noise, and Brownian motion

Abstract – We calculate the effective long-term convective velocity and dispersive motion of an ellipsoidal Brownian particle in three dimensions when it is subjected to a constant external force. This long-term motion results as a "net" average behavior from the particle rotation and translation on short time scales. Accordingly, we apply a systematic multi-scale technique to derive the effective equations of motion valid on long times. We verify our theoretical results by comparing them to numerical simulations.

Introduction. – The Brownian motion [1,2] of small particles suspended in an (aqueous) solvent, driven by the erratic impacts from the solvent molecules, is an ubiquitous phenomenon below micrometer length scales. Its theoretical foundations have been studied for over 100 years, with huge impact on the natural sciences in general and on physics in particular [3,4]. Still, there are many puzzles of surprisingly fundamental nature which are not yet fully resolved. An important example is the effect of hydrodynamic coupling between the translation and rotation of particles with arbitrary, non-spherical shape, like colloidal particles, colloidal clusters, DNA, proteins, nanotubes etc., on their overall diffusive behavior. This problem has recently attracted considerable interest [5–12], presumably spurred by the developments in single-particle tracking techniques which are able to record both, position and orientation, with high precision [5,6,12–16].

Brownian motion of non-spherical particles is characterized by a crossover from short-term anisotropic diffusion, dominated by the initial particle orientation, to effective "net" diffusion on very long times. For free Brownian motion without external forces, this behavior has been studied in some detail and is quite well understood [5,7–9]. The situation is different, however, if the diffusive motion is driven by an external force. The only theoretical studies in that direction, that we are aware of, are a recent analysis of driven Brownian motion of an asymmetrical particle in the plane [10], and a work by Brenner published in 1981 and little noted in the physical literature [17]. Having in mind the settling of a dilute suspension of small ellipsoidal particles due to gravitation, Brenner studied this problem under the term "sedimentation dispersion". However, for calculating this dispersion, *i.e.* the *effective long-term diffusion coefficient*, from the full description of particle translation and orientation, Brenner used what he himself calls an "*ad hoc* approach", and which in fact is not explained in any detail in [17].

In the present paper we analyze the effective long-term motion of a Brownian ellipsoidal particle in three dimensions, using a systematic multi-scale perturbation scheme. This scheme does not require an explicit parametrization of rotations in three dimensions, but can rather be performed on a relatively general and abstract level. We are thus able to fully recover the pioneering results by Brenner using an approach which over the last decades has become more established, and which opens up the prospect for further generalizations. We furthermore compare our results to numerical simulations of the coupled equations of motion for translation and rotation, as far as we know for the first time.

(a) E-mail: eichhorn@nordita.org

Model. – We model the dynamics of the Brownian ellipsoid by the force and torque balance relations

$$0 = -\gamma\dot{\boldsymbol{x}} + \boldsymbol{f} + \sqrt{2k_{\mathrm{B}}T}\gamma^{1/2}\boldsymbol{\xi}(t), \tag{1a}$$

$$0 = -\eta\boldsymbol{\omega} + \sqrt{2k_{\mathrm{B}}T}\eta^{1/2}\boldsymbol{\zeta}(t). \tag{1b}$$

The right-hand sides comprise all (non-inertial) forces and torques which add up to zero, because we neglect inertia effects [18,19] (overdamped approximation). The term $-\gamma\dot{\boldsymbol{x}}$ represents the viscous friction force acting on the particle center $\boldsymbol{x} = (x_1, x_2, x_3)$, given by the particles' translational velocity $\dot{\boldsymbol{x}}$ multiplying the friction tensor γ. All the externally applied forces are collected in $\boldsymbol{f} = (f_1, f_2, f_3)$. Throughout this paper, we consider only *constant* external force fields $\boldsymbol{f}$, independent of particle position and orientation. The last term in (1a) models the thermal fluctuations by unbiased Gaussian white-noise sources $\boldsymbol{\xi}(t) = (\xi_1(t), \xi_2(t), \xi_3(t))$ with correlations $\langle\xi_i(t)\xi_j(t')\rangle = \delta_{ij}\delta(t-t')$. The strength of these fluctuations is characterized by the thermal energy $k_{\mathrm{B}}T$ (k_{B} is Boltzmann's constant and T the temperature) and the friction tensor. Since γ is symmetric and positive definite, its square root $\gamma^{1/2}$ is uniquely defined, *i.e.* $\gamma^{1/2}\gamma^{1/2} = \gamma$. The thermal environment is assumed to be homogeneous, so that T and γ are constant in space. In (1b), all quantities represent the rotational counterparts to the ones from (1a), with the (positive definite and symmetric) rotational friction tensor η (independent of position $\boldsymbol{x}$), its square root $\eta^{1/2}$, the angular velocity $\boldsymbol{\omega}$, and unbiased Gaussian noise sources $\boldsymbol{\zeta}(t)$ which are independent of $\boldsymbol{\xi}(t)$. We restrict ourselves to the case without externally applied torques so that only viscous friction and thermal fluctuations contribute to the torque balance.

In principle, the dynamics of the Brownian ellipsoid is not fully specified yet by eqs. (1). While the force balance (1a) indeed represents an equation of motion for the translational Brownian movement of the center of the ellipsoid (overdamped Langevin equation [2,20]), the torque balance (1b) is a kinematic relation for the momentary angular velocity induced by the acting torques. For a full description, it has to be supplemented by a representation of the particle orientation and its equation of motion. As (1) is written in the laboratory frame, the friction tensors γ and η then directly depend on the parameters specifying the particle orientation, *i.e.* eqs. (1) are coupled. Common representations of rotations in three dimensions include Euler angles [21], quaternions [22] and unit vectors ("directors") attached to the particle [7,17,23]. It turns out, surprisingly, that the analysis we are going to present in the following can be performed without choosing a specific representation of orientation, so that the description provided by eqs. (1) is sufficient for our purposes.

As already mentioned in the Introduction, the driven diffusive motion of the ellipsoid described by (1) shows a crossover from short-term anisotropic behavior, dictated by the particle's initial orientation, to effective long-term convection and diffusion, after the initial orientation has been "forgotten". This crossover is characterized by the time it takes the particle to diffusively perform a full rotation. We can estimate it as $\tau_c = 1/\bar{Q}$, with $\bar{Q} = \mathrm{Tr}(\mathsf{Q})/3$ and $\mathsf{Q} = k_{\mathrm{B}}T\eta^{-1}$ the rotation diffusion tensor [11]. Being the average of the eigenvalues of Q, the choice of $\bar{Q}$ as a "net" rotational diffusion is physically intuitive. The length scale l_c associated with τ_c is given by the typical distance the particle covers by convection and diffusion during τ_c, *i.e.* $l_c = \max\{\tau_c|\boldsymbol{f}|\mathrm{Tr}(\gamma^{-1})/3\,,\ \sqrt{\tau_c\bar{D}}\}$, where we again used averaged friction and diffusion coefficients, in particular $\bar{D} = \mathrm{Tr}(\mathsf{D})/3 = k_{\mathrm{B}}T\mathrm{Tr}(\gamma^{-1})/3$ with the translation diffusion tensor $\mathsf{D} = k_{\mathrm{B}}T\gamma^{-1}$.

On time and length scales τ_L and L, much larger than τ_c and l_c, the ellipsoid will perform an "effective" translational motion, incorporating its rotational diffusion in an averaged way. We can therefore define the small dimensionless parameter

$$\varepsilon = \tau_c/\tau_L \ll 1 \tag{2}$$

to quantify the separation of the small scales τ_c and l_c from the large scales τ and L. Note that the long scales do not directly appear in the model (1), but rather are introduced by the question we ask: What is the effective long-term dynamics of the ellipsoid after transients have died out? This is unlike other typical problems involving distinct scales, where these scales are inherent to the problem so that a small (or large) parameter explicitly appears already in the equations of motion [23–25]. Nevertheless, also in the present case the standard multi-scale or homogenization technique [26–28] can be applied as a systematic perturbation procedure to derive the sought effective equations.

Multi-scale analysis. – The starting point of the multi-scale analysis is the (forward) Fokker-Planck equation for the probability density p that the ellipsoid has a certain position and orientation at time t [2,29,30]:

$$\frac{\partial p}{\partial t} - \left(\mathcal{L}^\dagger + \mathcal{M}^\dagger\right)p = 0, \tag{3a}$$

with

$$\mathcal{L}^\dagger = -\frac{\partial}{\partial x_i}\left[\left(\gamma^{-1}\boldsymbol{f}\right)_i - \frac{\partial}{\partial x_j}D_{ij}\right]. \tag{3b}$$

Here, we use the index notation and the summation convention to sum over repeated indices; D_{ij} are the components of the diffusion tensor D. The operator $\mathcal{M}^\dagger$ in (3a) represents the generator of rotary diffusion and thus involves the Laplace operator in rotation space whose specific form depends on the choice of parametrization of orientation. It is clear that this Fokker-Planck equation resolves the probability density on all scales. The essential step to disentangle small and large scales is to explicitly introduce them as *independent* variables and to presume that p is a function of all these variables. Using the symbol $\boldsymbol{\alpha}$ for collecting the three parameters representing orientation (without specifying them in any further detail), we

define

$$\tilde{\boldsymbol{x}} = \varepsilon^0 \boldsymbol{x}, \qquad \boldsymbol{X} = \varepsilon^1 \boldsymbol{x}, \qquad \tilde{\boldsymbol{\alpha}} = \varepsilon^0 \boldsymbol{\alpha}, \tag{4a}$$

and

$$\theta = \varepsilon^0 t, \qquad \vartheta = \varepsilon^1 t, \qquad \tau = \varepsilon^2 t, \tag{4b}$$

and require that

$$p = p(\theta, \vartheta, \tau, \tilde{\boldsymbol{x}}, \boldsymbol{X}, \tilde{\boldsymbol{\alpha}}). \tag{5}$$

With these definitions, $\boldsymbol{X}$ is of order one only for very large $\boldsymbol{x}$, and thus represents the large scale, which we are interested in. Likewise, the time variables ϑ and τ become of order one at large times t, where we expect from their relative scaling with respect to $\boldsymbol{X}$ that on ϑ scales long-term convective motion occurs and on τ scales long-term diffusive motion. The small-scale variables $\tilde{\boldsymbol{x}}$ and $\tilde{\boldsymbol{\alpha}}$ essentially correspond to the original variables $\boldsymbol{x}$ and $\boldsymbol{\alpha}$, but are restricted to small scales by imposing periodic boundary conditions for p, eq. (5), in $\tilde{\boldsymbol{x}}$ and $\tilde{\boldsymbol{\alpha}}$. The spatial periodicity is assumed to be l_c, whereas the small rotational scales $\tilde{\boldsymbol{\alpha}}$ are obviously periodic by definition. Relevant rotational motion occurs on small scales only. Accordingly, there is no large-scale rotational variable defined in (4a), and the long-term effective equations of motion will not include rotational degrees of freedom explicitly.

As a consequence of (4) and (5), the time and spatial derivatives in (3) turn into

$$\frac{\partial}{\partial t} = \frac{\partial}{\partial \theta} + \varepsilon \frac{\partial}{\partial \vartheta} + \varepsilon^2 \frac{\partial}{\partial \tau}, \quad \frac{\partial}{\partial x_i} = \frac{\partial}{\partial \tilde{x}_i} + \varepsilon \frac{\partial}{\partial X_i}, \tag{6}$$

while the generator of the rotational diffusion $\mathcal{M}^\dagger$ remains unchanged, in particular it does not involve any terms containing ε. In view of the scale separation (2) we can treat ε as a small perturbative parameter and expand p in powers of ε,

$$p = p^{(0)} + \varepsilon p^{(1)} + \varepsilon^2 p^{(2)} + \dots, \tag{7}$$

where all $p^{(i)}$ *a priori* inherit the functional dependence (5) on the various variables. In these variables, $p^{(0)}$ is normalized to one, while all other $p^{(i)}$ with $i > 0$ are normalized to zero. Plugging (6) and (7) into (3), and collecting terms of equal powers in ε in the resulting expression, we obtain a hierarchy of inhomogeneous Fokker-Planck–like equations of which we list the first three (order ε^0, ε^1 and ε^2):

$$\frac{\partial p^{(0)}}{\partial \theta} - \left(\tilde{\mathcal{L}}^\dagger + \tilde{\mathcal{M}}^\dagger\right) p^{(0)} = 0, \tag{8a}$$

$$\frac{\partial p^{(1)}}{\partial \theta} - \left(\tilde{\mathcal{L}}^\dagger + \tilde{\mathcal{M}}^\dagger\right) p^{(1)} = -\frac{\partial p^{(0)}}{\partial \vartheta} - \frac{\partial}{\partial X_i} v_i p^{(0)} + 2 \frac{\partial}{\partial \tilde{x}_i} \frac{\partial}{\partial X_j} D_{ij} p^{(0)}, \tag{8b}$$

$$\frac{\partial p^{(2)}}{\partial \theta} - \left(\tilde{\mathcal{L}}^\dagger + \tilde{\mathcal{M}}^\dagger\right) p^{(2)} = -\frac{\partial p^{(0)}}{\partial \tau} - \frac{\partial p^{(1)}}{\partial \vartheta} - \frac{\partial}{\partial X_i} v_i p^{(1)} + \frac{\partial}{\partial X_i} \frac{\partial}{\partial X_j} D_{ij} p^{(0)} + 2 \frac{\partial}{\partial \tilde{x}_i} \frac{\partial}{\partial X_j} D_{ij} p^{(1)}. \tag{8c}$$

In (8), we introduce the velocity vector $\boldsymbol{v} = \gamma^{-1} \boldsymbol{f}$ and the tilde over the operators $\tilde{\mathcal{L}}^\dagger$ and $\tilde{\mathcal{M}}^\dagger$ to indicate that they act on the small-scale variables $\tilde{\boldsymbol{x}}$ and $\tilde{\boldsymbol{\alpha}}$, respectively. Note that (8a) is *exactly the same* equation as (3a), with the essential difference, however, that $p^{(0)}$ obeys *periodic* boundary conditions in the variables $\tilde{\boldsymbol{x}}$ and $\tilde{\boldsymbol{\alpha}}$.

For finding the solutions of the equation hierarchy (8) we largely follow the standard procedure detailed, *e.g.*, in [28] (see also [31]). We are interested in solutions of (8) which are stationary on small scales after short-term transients have died out. Hence, the desired solutions do not depend on θ such that we can set $\partial p^{(i)}/\partial \theta = 0$ for all i. A further important observation is that $\tilde{\mathcal{M}}^\dagger$ and $\tilde{\mathcal{L}}^\dagger$ do not depend on the large-scale variable $\boldsymbol{X}$. The solution to (8a) is therefore given by a product ansatz

$$p^{(0)} = w(\tilde{\boldsymbol{x}}, \tilde{\boldsymbol{\alpha}}) \rho^{(0)}(\vartheta, \tau, \boldsymbol{X}), \tag{9}$$

where w has to be normalized over $\tilde{\boldsymbol{x}}$ and $\tilde{\boldsymbol{\alpha}}$, and $\rho^{(0)}$ over $\boldsymbol{X}$. Exploiting that $\boldsymbol{v}$ in $\tilde{\mathcal{L}}^\dagger$ is constant in space and that dependencies on particle orientation enter only via γ^{-1} (likewise in $\tilde{\mathcal{M}}^\dagger$ where the rotational diffusion coefficient depends on orientation via η^{-1}), we find w to be uniform for all $\tilde{\boldsymbol{x}}$ and $\tilde{\boldsymbol{\alpha}}$, with a constant value set by normalization: $w = 1/(4\pi l_c^3)$. This uniform distribution carries a probability current $\boldsymbol{v}w$ (see (3b)), corresponding to an averaged particle velocity

$$\boldsymbol{V} = \int \mathrm{d}\tilde{\boldsymbol{x}} \mathrm{d}\tilde{\boldsymbol{\alpha}}\, \boldsymbol{v} w = \overline{\gamma^{-1} \boldsymbol{f}} = \overline{\gamma^{-1}} \boldsymbol{f}, \tag{10}$$

where the overbar denotes the average over the uniform orientational distribution.

Solving eqs. (8b) and (8c) is a little more involved because of the inhomogeneities on the right-hand sides. For a non-trivial solution to exist, they have to fulfill a so-called solvability condition [28], stating that these inhomogeneities have to be orthogonal to the null-space of the operator $\tilde{\mathcal{M}} + \tilde{\mathcal{L}}$ adjoint to $\tilde{\mathcal{M}}^\dagger + \tilde{\mathcal{L}}^\dagger$. The nullspace of $\tilde{\mathcal{M}} + \tilde{\mathcal{L}}$ contains all constants (in $\tilde{\boldsymbol{x}}$ and $\tilde{\boldsymbol{\alpha}}$), so that the solvability condition for (8b) reads $\int \mathrm{d}\tilde{\boldsymbol{x}} \mathrm{d}\tilde{\boldsymbol{\alpha}} \left(-\frac{\partial p^{(0)}}{\partial \vartheta} - \frac{\partial}{\partial X_i} v_i p^{(0)} + 2 \frac{\partial}{\partial \tilde{x}_i} \frac{\partial}{\partial X_j} D_{ij} p^{(0)}\right) = 0$. Inserting our above result (9) for $p^{(0)}$, we find

$$\frac{\partial \rho^{(0)}}{\partial \vartheta} + \frac{\partial}{\partial X_i} V_i \rho^{(0)} = 0. \tag{11}$$

With this equation (and using $p^{(0)} = w\rho^{(0)}$) we can simplify (8b) to

$$\left(\tilde{\mathcal{M}}^\dagger + \tilde{\mathcal{L}}^\dagger\right) p^{(1)} = w(v_i - V_i) \frac{\partial \rho^{(0)}}{\partial X_i}. \tag{12}$$

As $w(v_i - V_i)$ is a function of the small-scale variables while $\partial \rho^{(0)}/\partial X_i$ depends on large scales only, we can solve (12) again by a product ansatz. We thus set

$$p^{(1)} = w \lambda_{ij}(\tilde{\boldsymbol{x}}, \tilde{\boldsymbol{\alpha}}) f_j \frac{\partial \rho^{(0)}}{\partial X_i}(\vartheta, \tau, \boldsymbol{X}), \tag{13}$$

where the factor w has been introduced for later convenience. Likewise, also the specific expression $\lambda_{ij} f_j = (\lambda \boldsymbol{f})_i$ for the unknown vector function of the small scales involving an auxiliary tensor $\lambda = \lambda(\tilde{\boldsymbol{x}}, \tilde{\boldsymbol{\alpha}})$ proves to be very convenient.

The ansatz (13) solves (12) provided that the functions λ_{ij} solve the auxiliary equation $(\tilde{\mathcal{L}}^\dagger + \tilde{\mathcal{M}}^\dagger)\lambda_{ij} f_j = v_i - V_i = (\gamma^{-1} - \overline{\gamma^{-1}})_{ij} f_j$, where we used the definition $\boldsymbol{v} = \gamma^{-1}\boldsymbol{f}$ and eq. (10) for rewriting the right-hand side inhomogeneity $v_i - V_i$ in the last step. Observing that this inhomogeneity, as well as all v_i and D_{ij} appearing in $\tilde{\mathcal{L}}^\dagger$, are independent of $\tilde{\boldsymbol{x}}$, we conclude that the λ_{ij} do not depend on $\tilde{\boldsymbol{x}}$ either, so that $(\tilde{\mathcal{L}}^\dagger + \tilde{\mathcal{M}}^\dagger)\lambda_{ij} f_j = \tilde{\mathcal{M}}^\dagger \lambda_{ij} f_j$. As λ_{ij} is supposed to be a solution for any (constant) $\boldsymbol{f}$, the above auxiliary equation thus simplifies to the tensor equation

$$\tilde{\mathcal{M}}^\dagger \lambda_{ij} = (\gamma^{-1})_{ij} - \overline{(\gamma^{-1})_{ij}}. \tag{14}$$

In addition, all λ_{ij} have to fulfill the "normalization"

$$\int \mathrm{d}\tilde{\boldsymbol{\alpha}}\, \lambda_{ij} = \overline{\lambda_{ij}} = 0 \tag{15}$$

to guarantee the overall normalization of p in (5).

Analogously to the above procedure for (8b), we next analyse the solvability condition for the second order equation (8c). Plugging in the results we derived so far, namely (9), (11) and (13), we obtain in a straightforward way

$$\frac{\partial \rho^{(0)}}{\partial \tau} - D_{ij}^{\mathrm{eff}} \frac{\partial}{\partial X_i} \frac{\partial}{\partial X_j} \rho^{(0)} = 0, \tag{16}$$

with the effective diffusion coefficient on large scales

$$D_{ij}^{\mathrm{eff}} = k_{\mathrm{B}} T\, \overline{(\gamma^{-1})_{ij}} - \overline{(\gamma^{-1})_{ik} \lambda_{jl}}\, f_k f_l, \tag{17}$$

where we used (15) to arrive at the given form of the second term.

As anticipated when introducing the scaling ansatz (4), the main results (11) and (16) of the multi-scale analysis consist in an equation, which describes convective motion with an effective velocity on time scales ϑ and large spatial scales (eq. (11)), and an equation, which governs diffusion with an effective diffusion coefficient on time scales τ and large spatial scales (eq. (16)). In order to combine them into one effective equation of motion, we switch back to the original variables t and $\boldsymbol{x}$, and use that the marginal density $\rho(t, \boldsymbol{x})$ in translation space only is obtained by integrating p over orientational degrees of freedom, $\rho = \int \mathrm{d}\boldsymbol{\alpha}\, p$. From (5) we conclude that $\rho = \rho^{(0)}$ in lowest order ε. Using (6) (and $\partial \rho^{(0)}/\partial \theta = 0$) we find $\partial \rho / \partial t = \varepsilon\, \partial \rho^{(0)}/\partial \vartheta + \varepsilon^2 \partial \rho^{(0)}/\partial \tau$ in lowest order. Plugging in our results (11) and (16), and noticing that $\boldsymbol{x} = \varepsilon^{-1}\boldsymbol{X}$ (see (4)) we finally arrive at

$$\frac{\partial \rho}{\partial t} + \frac{\partial}{\partial x_i}\left(V_i - D_{ij}^{\mathrm{eff}} \frac{\partial}{\partial x_j} \right) \rho = 0. \tag{18}$$

Although it is given in the original variables t and $\boldsymbol{x}$, we know from the way it has been derived that this effective forward Fokker-Planck equation is a valid description of the dynamics of our system (1) only in the long-term regime $t \gg \tau_c$ and $|\boldsymbol{x}| \gg l_c$. As usual in multi-scale schemes [28], the explicit expressions for the "effective coefficients" V_i and D_{ij}^{eff} are obtained from solving an auxiliary equation on the small scales, here eq. (14), and from averaging over these small scales (see eqs. (10) and (17)).

Calculation of the effective coefficients. – The relevant averages over small-scale rotational variables in (10), (14) and (17) are of the form $\overline{(\gamma^{-1})_{ij}}$ and $\overline{(\gamma^{-1})_{ik}\lambda_{jl}}$. Since these averages are performed over a uniform distribution of orientations, the resulting tensors should be invariant under rotation. We can thus use invariance theory to show that

$$\overline{(\gamma^{-1})_{ij}} = \frac{1}{3}\mathrm{Tr}(\gamma^{-1})\delta_{ij}, \tag{19a}$$

$$\overline{(\gamma^{-1})_{ik}\lambda_{jl}} = \left[-\frac{1}{15}\delta_{ik}\delta_{jl} + \frac{1}{10}(\delta_{ij}\delta_{kl} + \delta_{il}\delta_{jk}) \right] \times \mathrm{Tr}(\gamma^{-1}\lambda). \tag{19b}$$

In analogy to (19a) we also find $\overline{\lambda_{ij}} = \delta_{ij}\mathrm{Tr}(\lambda)/3$, so that λ has to be traceless according to (15). The property $\mathrm{Tr}(\lambda) = 0$ has already been used to simplify (19b).

In order to find the solution to the auxiliary equation (14), we first rewrite its right-hand inhomogeneity using (19a),

$$(\hat{\gamma}^{-1})_{ij} = (\gamma^{-1})_{ij} - \frac{1}{3}\mathrm{Tr}(\gamma^{-1})\delta_{ij}, \tag{20}$$

i.e. $(\hat{\gamma}^{-1})_{ij}$ denotes the traceless part of the inverse friction tensor. This tensor $(\hat{\gamma}^{-1})_{ij}$ depends on the particle orientation via rotation matrices $\mathsf{R} = \mathsf{R}(\boldsymbol{\alpha})$, *i.e.* $(\hat{\gamma}^{-1})_{ij} = (\mathsf{R}\hat{\Gamma}^{-1}\mathsf{R}^{\mathsf{T}})_{ij}$, where the traceless inverse friction tensor $\hat{\Gamma}^{-1}$ represents an arbitrary reference configuration and thus is constant. Typically, it is chosen such that the principal axes of the ellipsoid are aligned with the coordinate axes of the laboratory frame, because then $\hat{\Gamma}_{ij}$ is diagonal. Assuming that the mobility tensor γ^{-1} and the rotational diffusion tensor Q appearing in $\mathcal{M}^\dagger$ can be diagonalized in the same frame, this is also the configuration of the ellipsoid in which Q (with components Q_{ij}) is diagonal. We may therefore expect that even λ_{ij} "inherits" that property such that it can be written as $\lambda_{ij} = (\mathsf{R}\Lambda\mathsf{R}^{\mathsf{T}})_{ij}$ with Λ being diagonal and constant.

To find the explicit form of the rotation matrices $\mathsf{R}(\boldsymbol{\alpha})$ and, in particular, the rotary diffusion operator $\mathcal{M}^\dagger$ for a specific parametrization of orientation may be quite cumbersome. However, in [32] Rallison showed that we can write

$$\mathcal{M}^\dagger = \epsilon_{ikl} R_{km} \frac{\partial}{\partial R_{lm}} Q_{ij} \epsilon_{jpq} R_{pn} \frac{\partial}{\partial R_{qn}}, \tag{21}$$

independently of the specific representation of rotation, as only derivatives $\partial/\partial R_{ij}$ with respect to the ij-component of the rotation matrix appear (ϵ_{ijk} is the Levi-Civita tensor). With this expression and the above ansatz for $(\hat{\gamma}^{-1})_{ij}$ and λ_{ij}, (14) reduces to an algebraic equation,

which is easily inverted. After some lengthy but straightforward algebra, we find the solution

$$\lambda_{ij} = \frac{1}{6\Delta}\left[\mathrm{Tr}(\mathsf{Q}\hat{\gamma}^{-1})\delta_{ij} - 3(\mathsf{Q}\hat{\gamma}^{-1})_{ij}\right], \tag{22a}$$

with

$$\Delta = Q^{(1)}Q^{(2)} + Q^{(2)}Q^{(3)} + Q^{(3)}Q^{(1)}, \tag{22b}$$

and the eigenvalues $Q^{(i)}$ of the rotary diffusion tensor Q.

Plugging the expressions (19) and (22a) into (10) and (17), we obtain the final results for the effective coefficients,

$$V_i = \frac{1}{3}\mathrm{Tr}(\gamma^{-1})f_i, \tag{23a}$$

$$D_{ij}^{\mathrm{eff}} = \bar{D}\,\delta_{ij} + \kappa_{ij}, \tag{23b}$$

where we re-used the abbreviation $\bar{D} = \mathrm{Tr}(\mathsf{D})/3 = k_{\mathrm{B}}T\mathrm{Tr}(\gamma^{-1})/3$ in (23b) and defined

$$\kappa_{ij} = \frac{1}{2\Delta}\mathrm{Tr}\left(\hat{\gamma}^{-1}\mathsf{Q}\hat{\gamma}^{-1}\right)\left(\frac{1}{30}f_if_j + \frac{1}{10}\boldsymbol{f}^2\delta_{ij}\right). \tag{23c}$$

For the specific choice $\boldsymbol{f} = (f, 0, 0)$, the effective diffusion tensor becomes diagonal with

$$\kappa_{11} = \frac{1}{15\Delta}\mathrm{Tr}\left(\hat{\gamma}^{-1}\mathsf{Q}\hat{\gamma}^{-1}\right)f^2, \quad \kappa_{22} = \kappa_{33} = \frac{3}{4}\kappa_{11}. \tag{24}$$

The 11-component quantifies effective diffusion parallel, and the 22- and 33-component perpendicular to the direction of the external force $\boldsymbol{f}$.

Numerical simulations. – We compare our main results (23) to numerical simulations of the original equations of motion (1) for a representative ellipsoid with ratio $1:2:3$ between its three semi-axes. For the simulations, we choose quaternions as a concrete parametrization of rotation, *i.e.* the model (1) is supplemented by the equation of motion for the quaternion q,

$$\dot{q} = \frac{1}{2}\omega \circ q, \tag{25}$$

where the symbol $\circ$ denotes a *quaternion* product [22] evaluated in the Stratonovich sense [2,29,30], and where ω is the angular velocity in the laboratory frame from (1b), represented as a pure quaternion [22]. We solve (1) and (25) using the Euler algorithm with time step 0.1 ms. The explicit values for the (eigenvalues of the) friction tensors γ and η of the ellipsoid are calculated from the exact expressions given in [33]. For the simulations we choose an ellipsoid with semi-axis lengths 0.3 μm, 0.6 μm and 0.9 μm. The results of the simulations averaged over 10000 realizations of the noise sources (with identical initial conditions) are shown in fig. 1. The crossover from short-term to long-term diffusion is clearly visible to occur at a time around the order of a second, well comparable to the estimation $\tau_c = 1/\bar{Q} = 1.4\,\mathrm{s}$. The long-term coefficients obtained from these simulations are in perfect agreement with the theoretical predictions (23).

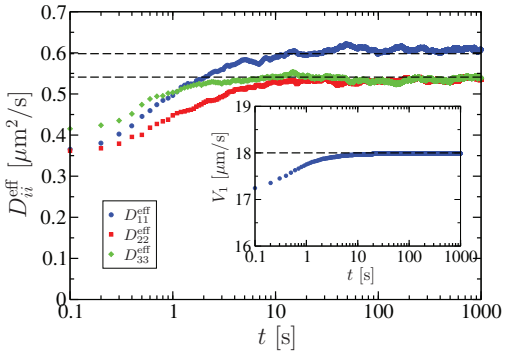

Fig. 1: (Colour online) Comparison of numerical simulations with the theoretical predictions (23). The symbols show the three different components of the net diffusion coefficients D_{ii}^{eff} and the net translational velocity V_1 (inset) as a function of time, averaged over 10000 realization of the Gaussian noise source, but for identical initial position and orientation of the ellipsoid. The dashed horizontal lines represent the theoretical long-term predictions from (23), $D_{11}^{\mathrm{eff}} = 0.60\,\mu\mathrm{m}^2/\mathrm{s}$, $D_{22}^{\mathrm{eff}} = D_{33}^{\mathrm{eff}} = 0.54\,\mu\mathrm{m}^2/\mathrm{s}$ and $V_1 = 0.18\,\mu\mathrm{m/s}$ (the other net velocity components are zero, not shown). For comparison, the purely thermal contribution to the net diffusion is $\bar{D} = 0.37\,\mu\mathrm{m}^2/\mathrm{s}$. The simulated ellipsoid has semi-axis lengths 0.3 μm, 0.6 μm and 0.9 μm. In water, its translational friction coefficients for moving in the direction of these axes are (to two digits precision) 12 fN s/μm, 11 fN s/μm, and 10 fN s/μm, respectively, and its friction coefficients for rotation around these axes are 7.1 fN μm s, 6.8 fN μm s, and 4.1 fN μm s [33]. The thermal energy is set to $k_{\mathrm{B}}T = 4.1$ fNμm, corresponding to room temperature (300 K). The external force is $\boldsymbol{f} = (200\,\mathrm{fN},\ 0\,\mathrm{fN},\ 0\,\mathrm{fN})$.

Discussion and conclusions. – The effective diffusion coefficient (23b) is composed of two contributions. The first one, $\bar{D}\delta_{ij}$, is the purely thermal diffusion of the center of the ellipsoid, averaged over all particle orientations. The second one, κ_{ij}, is a dispersion effect stemming from the variations of the translational velocity with diffusive changes of the particle orientation relative to the direction of the external force $\boldsymbol{f}$. This contribution is anisotropic, the dispersion effect is stronger in the direction of the force than perpendicular to it. Remarkably, the ratio 4/3 between the parallel and perpendicular component (see (24)) is completely independent of the specific shape of the ellipsoid. Furthermore, this anisotropy is only present in three dimensions. For two dimensions, the effective diffusion tensor analogous to (23c) turns out to be *isotropic*; it has been obtained in [10] by formally solving the Langevin equations of motion for translation and rotation in the plane.

It is straightforward to verify that (23b) and (24) agree with the results obtained by Brenner in [17]. However, unlike [17] we have here shown that (18) and (23) follow from a rigorous perturbative multi-scale technique which has been widely used in physics and applied mathematics over the last 10–20 years. Mean convective velocity and effective diffusion tensor are both computed by solving an auxiliary equation (see eq. (14)), and by performing

averages over the stationary rotational distribution of the original model (see eqs. (19)). In the case studied here, where there is no torque, this procedure is pretty straightforward: the stationary rotational distribution is uniform, and the solution of the auxiliary equation can be obtained by a simple ansatz. In more general settings, the stationary distribution as well as the solution of the auxiliary equation would have to be computed numerically, in analogy to the description of scalar transport in compressible flows presented in [26]; we will leave this for future work. Specifically, such more general settings may include external torques [34,35], or other types of external "forces", like hydrodynamic flows or phoretic mechanisms which drive particle motion. We finally remark that experiments for measuring the long-term convective and diffusive motion of ellipsoidal particles in three dimensions, and for verifying our theoretical predictions in (23), could be performed along the lines of [12,14].

* * *

Financial support by the Swedish Science Council (Vetenskapsrådet) under the grants 621-2012-2982 and 621-2013-3956 is acknowledged.

REFERENCES

[1] Duplantier B., in *Einstein, 1905-2005: Poincaré Seminar 2005, Progress in Mathematical Physics*, Vol. **47** (Birkhäuser Verlag, Basel) 2005, pp. 201–293.
[2] Mazo R. M., *Brownian Motion: Fluctuations, Dynamics and Applications* (Oxford University Press, Oxford) 2002.
[3] Frey E. and Kroy K., *Ann. Phys. (Leipzig)*, **14** (2005) 20.
[4] Hänggi P. and Marchesoni F., *Chaos*, **15** (2005) 026101.
[5] Han Y., Alsayed A. M., Nobili M., Zhang J., Lubensky T. C. and Yodh A. G., *Science*, **314** (2006) 626.
[6] Han Y., Alsayed A., Nobili M. and Yodh A. G., *Phys. Rev. E*, **80** (2009) 011403.
[7] Gonzalez O. and Li J., *SIAM J. Appl. Math.*, **70** (2010) 2627.
[8] Cichocki B., Ekiel-Jezewska M. L. and Wajnryb E., *J. Chem. Phys.*, **136** (2012) 071102.
[9] Cichocki B., Ekiel-Jezewska M. L. and Wajnryb E., *J. Chem. Phys.*, **142** (2015) 214902.
[10] Grima R. and Yaliraki S. N., *J. Chem. Phys.*, **127** (2007) 084511.
[11] Ribrault C., Triller A. and Sekimoto K., *Phys. Rev. E*, **75** (2007) 021112.
[12] Kraft D., Wittkowski R., ten Hagen B., Edmond K. V., Pine D. J. and Löwen H., *Phys. Rev. E*, **88** (2013) 050301(R).
[13] Fung J., Martin K. E., Perry R. W., Kaz D. M., McGorty R. and Manoharan V. N., *Opt. Express*, **19** (2011) 8051.
[14] Fung J. and Manoharan V. N., *Phys. Rev. E*, **88** (2013) 020302(R).
[15] Chakrabarty A., Konya A., Wang F., Jonathan V., Selinger J. V., Sun K. and Wei Q.-H., *Phys. Rev. Lett.*, **111** (2013) 160603.
[16] Chakrabarty A., Konya A., Wang F., Jonathan V., Selinger J. V., Sun K. and Wei Q.-H., *Langmuir*, **30** (2014) 13844.
[17] Brenner H., *J. Colloid Interface Sci.*, **80** (1981) 548.
[18] Purcell E. M., *Am. J. Phys.*, **45** (1977) 3.
[19] Dusenbery D. B., *Living at Micro Scale* (Harvard University Press, Cambridge, Mass.) 2011.
[20] Snook I., *The Langevin and Generalised Langevin Approach to the Dynamics of Atomic, Polymeric and Colloidal Systems* (Elsevier, Amsterdam) 2007.
[21] Goldstein H., *Classical Mechanics* (Addison-Wesley, New York) 1980.
[22] Coutsias E. A. and Romero L., *The Quaternions with Applications to Rigid Body Dynamics*, Sandia National Laboratories, Technical Report SAND2004-0153 (2004).
[23] Marino R., Eichhorn R. and Aurell E., *Phys. Rev. E*, **93** (2016) 012132.
[24] Pagitsas M., Nadim A. and Brenner H., *Physica*, **135A** (1986) 533.
[25] Mazzino A., Musacchio S. and Vulpiani A., *Phys. Rev. E*, **71** (2005) 011113.
[26] Vergassola M. and Avellaneda M., *Physica D*, **106** (1997) 148.
[27] Bender C. and Orszag S. A., *Advanced Mathematical Methods For Scientists and Engineers: Asymptotic Methods and Perturbation Theory* (Springer, New York) 1999.
[28] Pavliotis G. A. and Stuart A. M., *Multiscale Methods: Averaging and Homogenization* (Springer, New York) 2008.
[29] Gardiner C. W., *Handbook of Stochastic Methods* (Springer, Berlin) 1983.
[30] van Kampen N. G., *Stochastic Processes in Physics and Chemistry* (North-Holland, Amsterdam) 1987.
[31] Marino R. and Aurell E., *Advective-diffusive motion on large scales from small-scale dynamics with an internal symmetry*, arXiv:1603.06823 (2016).
[32] Rallison J. M., *J. Fluid Mech.*, **84** (1978) 237.
[33] Brenner H., *J. Colloid Interface Sci.*, **23** (1967) 407.
[34] Güell O., Tierno P. and Sagués F., *Eur. Phys. J. Special Topics*, **187** (2010) 15.
[35] Sandoval M., *Phys. Rev. E*, **87** (2013) 032708.